IOP Conference Series:
Earth and
Environmental Science

PAPER • **OPEN ACCESS**

Preliminary Evaluation of The Cyprus Erythemal Irradiance Forecasting System

To cite this article: G Charalampous *et al* 2025 *IOP Conf. Ser.: Earth Environ. Sci.* **1522** 012038

Preliminary Evaluation of The Cyprus Erythemal Irradiance Forecasting System

G Charalampous[1,2*], K Fragkos[1], A Nisantzi[1,2], I Fountoulakis[3,4], K Papachristopoulou[3,5], D Hadjimitsis[2,1] and S Kazadzis[5]**

[1] Department of Resilience Society, Eratosthenes Centre of Excellence, Limassol, Cyprus
[2] Department of Civil Engineering & Geomatics, Cyprus University of Technology, Limassol, Cyprus
[3] Institute for Astronomy, Astrophysics, Space Applications and Remote Sensing, National Observatory of Athens (IAASARS/NOA), Athens, Greece
[4] Research Centre for Atmospheric Physics and Climatology, Academy of Athens, Athens, Greece
[5] Physikalisch-Meteorologisches Observatorium Davos, World Radiation Center, Davos, Switzerland
** Current affiliation: Climate and Atmosphere Research Center, the Cyprus Institute, Konstantinou Kavafi 20, 2121 Aglantzia, Nicosia, Cyprus

[*]E-mail: georgia.charalambous@eratosthenes.org.cy

Abstract. Cyprus experiences some of the highest levels of solar radiation in Europe, which presents both opportunities for solar energy and risks associated with ultraviolet (UV) exposure. In response to the need for better public awareness and UV protection measures, the Cyprus Erythemal Irradiance Forecasting System (CERYFOS) was developed to forecast the UV Index (UVI) across the island. This paper presents a preliminary evaluation of the CERYFOS model's accuracy by comparing forecasted UVI values with ground-based measurements taken from December 2023 to September 2024. The model's predictions were assessed against data from a Kipp & Zonen SUV-E actinometer and a Bentham DMc150 spectrophotometer, operating in Limassol. Results showed that the system performs well under clear-sky conditions, achieving a Root Mean Squared Error (RMSE) of 0.36[UVI units] and minimal bias. The study also highlights the influence of aerosol optical depth (AOD) and ozone variability on forecast accuracy. These findings underline the need for model refinements, particularly concerning cloud impact and atmospheric parameter representation. With further improvements, CERYFOS has the potential to enhance public safety by providing accurate UVI forecasts and increasing awareness of UV exposure risks in Cyprus.

1. Introduction

The Ultraviolet Index (UVI) is a simple yet effective metric, presented on a colour scale from 0 to 10+, that indicates the intensity of ultraviolet (UV) radiation reaching the Earth's surface. This index serves as a critical indicator for potential skin damage due to UV exposure. Initially developed by scientists from Environment Canada in 1992, the UVI was later adopted by both the World Meteorological Organization (WMO) and the World Health Organization (WHO) as a tool to help individuals reduce the risks associated with overexposure to the sun [1]. These risks include acute effects like sunburn, as well as long-term impacts such as premature skin aging and an increased risk of skin cancers, including basal cell carcinoma, squamous cell carcinoma, and melanoma [2]. Furthermore, excessive exposure to UV radiation is a leading cause of ocular conditions such as cataracts [3] and can also weaken the immune system [4], reducing the body's ability to fight infections.

Many European countries provide forecasts of the UVI, which are readily available to the public to help manage sun exposure [5]. The European UV-Index Initiative (http://www.uv-index.org/) further enhances accessibility to UVI data by offering a platform that consolidates online UV measurements, improves visualization, and ensures data quality.

In Cyprus, the European country with the highest levels of sunshine, there is currently no dedicated national UV-Index forecasting system. To address this gap and promote awareness of optimal sun exposure, we developed the Cyprus Erythemal Forecasting System (CERYFOS) in December 2023. Given that a significant portion of the Cypriot population, particularly those with lower educational backgrounds, does not adhere to appropriate protective measures when exposed to the sun [6], this platform aims to provide reliable UVI forecasts and serve as an educational tool for the public.

In this paper, we present an initial evaluation of the CERYFOS platform's forecasts by comparing them with ground-based UVI measurements. The structure of the paper is as follows: Section 2 details the forecasting system, the instruments, and the methodology used for evaluation. Section 3 presents the results of the preliminary evaluation and discusses the key factors contributing to the observed discrepancies between forecasts and measurements. Finally, Section 4 provides a summary of the main conclusions and suggests areas for future improvements based on this initial evaluation.

2. CERYFOS Forecasting System

2.1 CERYFOS Platform Description

The Cyprus Erythemal Irradiance Forecasting System (CERYFOS) is a collaborative effort involving the Eratosthenes Centre of Excellence, the National Observatory of Athens, and the Physikalisch-Meteorologisches Observatorium Davos World Radiation Center. CERYFOS provides hourly UVI forecasts for the next two days with a spatial resolution of 0.1x0.1 degrees. The system uses the radiative transfer model libRadtran [7][8], incorporating data from various sources to generate accurate forecasts under clear sky conditions. Forecasts for all-sky conditions are subsequently produced by applying Cloud Modification Factors (CMFs) derived from the Weather Research and Forecasting (WRF) model.

The Key data inputs for the UVI forecasting system include:

1. **Cloud Forecasts**: Derived from the WRF model, these forecasts provide CMFs, which are calculated as the ratio between all-sky and clear-sky surface solar radiation values from the WRF model. The CMFs are generated hourly with a high spatial resolution of 2x2 km, allowing for detailed cloud impact assessments on surface UV radiation.

2. **Aerosol Optical Properties**: Sourced from the Copernicus Atmosphere Monitoring Service (CAMS), the primary aerosol inputs include the forecasted Aerosol Optical Depth at 550 nm (AOD550), single scattering albedo at 550 nm, and the Ångström exponent (AE). These parameters are crucial for accurately modeling aerosol effects on UV

radiation. The forecasts for the day of interest are values from the CAMS "global atmospheric composition forecasts" [9][10]with a spatial resolution of 40 km.

3. **Total Ozone Column Data**: Provided by the Tropospheric Emission Monitoring Internet Service (TEMIS) at a spatial resolution of 1x1 degrees [11], this dataset supplies total column ozone values essential for calculating surface UV radiation, given that ozone concentration strongly influences the UVI.
4. **Surface Elevation Data**: Obtained from a high-resolution Digital Elevation Model (DEM) provided by NOAA, this dataset allows the model to adjust UVI calculations based on altitude, addressing the increase in UV radiation exposure with elevation.

The UVI forecasting platform is accessible via the UVI Nexus Hub, offering users the ability to view daily UV forecasts for major cities in Cyprus, including Nicosia, Limassol, Paphos, Larnaca, and Famagusta. To accommodate diverse user needs, forecasts are available in multiple formats: interactive maps, bar plots, and tables. This versatility ensures accessibility and ease of interpretation for both general and specialized audiences. For a comprehensive description of the forecasting methodology and the platform's architecture, see [12].

2.2 Methodology

To evaluate the performance of CERYFOS, a validation study was conducted by comparing the model's UVI predictions with actual measurements from a Kipp & Zonen SUV-E radiometer installed in Limassol Cyprus. Data collection spanned from December 2023 to September 2024, and measurements were taken under all weather conditions. Additionally, measurements from an all-sky imager type EKO ASI-16 for identifying the clear sky periods and a double monochromator Bentham DMc150 spectrophotometer were used to evaluate the quality of the radiometer's data. An overview of the instrumentation is given in [13].

The methodology involved correcting the spectral misalignment of the radiometer (difference of instrument spectral response with the Erythema reference action spectrum) due to varying ozone levels retrieved from the Ozone Monitoring Instrument (OMI), and zenith angles [14]. Forecasted data, such as, aerosol optical depth (AOD), and ozone column levels, were compared with ground-based measurements of AOD from the Aerosol Robotic Network (AERONET), at 550 nm and with actual ozone measurements sourced from the Ozone Monitoring Instrument (OMI) overpass data, to verify the accuracy of the input parameters in the radiative transfer model, and their impact on the forecast system performance. For more accurate assessment, clear sky conditions were identified using images from an All-Sky camera at the Limassol station as well. Key statistical measures, such as Mean Bias Error (MBE), Root Mean Squared Error (RMSE), were used to evaluate the model's predictive accuracy.

2.3 Measurement Traceability and Uncertainty

The instruments used for this study follow a strict calibration and maintenance protocol to ensure the traceability and accuracy of measurements. The SUV-E radiometer was accompanied with a calibration certificate upon its purchase. The calibration by the provider is traceable to the Dutch national metrology laboratory (VSL B.V.), which ensures high accuracy with a calibration uncertainty (k=2) of ±2.4%.

To address spectral mismatch errors between the instrument's real response and the ideal erythema action spectrum, the mean sensitivity (χ) of 26 $(W/m^2)/V$ is weighted with appropriate scaling factors that have been calculated using a radiative transfer model over a range of solar zenith angles (0°–70°) and ozone columns (260–400 DU). This sensitivity matrix reduces errors (-7.2% to 2.8%) when applied to match specific atmospheric conditions. Regular validation procedures, such as those recommended by Kipp & Zonen, minimize deviations and maintain the integrity of the instrument's performance. Comparison between nearly synchronous measurements from the SUV-E and the Bentham spectroradiometer further ensures the reliability of both datasets. Accurate quantification of the overall uncertainty in the SUV-E measurements considering all uncertainty sources (calibration, spectral mismatch, imperfect angular response, etc.) has not been performed yet, though according to the provider the overall uncertainty for SZA below 70° is of the order of 5%.

For the Bentham Spectroradiometer, a rigorous traceability chain has been established to ensure accuracy. Monthly calibrations involve the use of Schreder CMS 200 W quartz halogen lamps that are traceable to the scale of Physikalisch-Technische Bundesanstalt (PTB), specifically aged and certified for their intended orientation and usage. These lamps, used in conjunction with the KS-J1011 portable field calibrator, provide an absolute spectral irradiance standard. Based on the existing literature [15] relative to the overall uncertainties in the measurements of such instruments. we estimate an overall uncertainty of less than 5%.

3. Results and Discussion

3.1 UVI all sky conditions

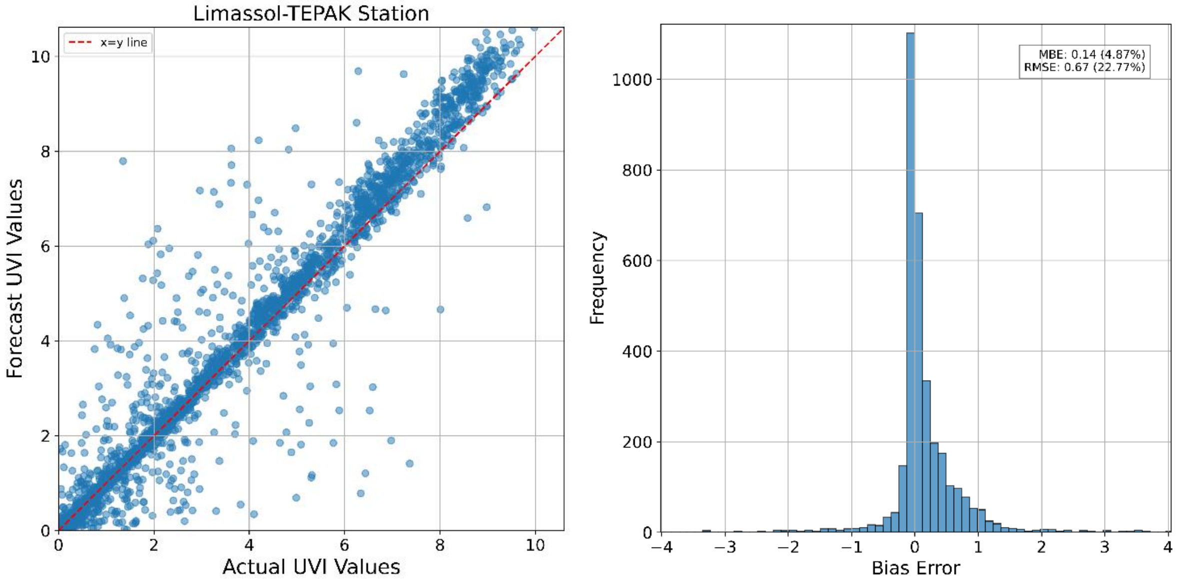

Figure 1. Comparison between forecasted and measured UV Index (UVI): (Left panel) Scatter plot of forecasted versus measured UVI values, and (Right panel) frequency distribution of the Bias Error (forecasted – measured UVI) for the period of December 2023 to September 2024, across all sky conditions.

Figure 1 presents the comparison between forecasted and measured UVI values under all-sky conditions for the period from December 2023 to September 2024. The model demonstrates generally good performance, as seen in the clustering of data points close to the 1:1 line (Figure

1, left panel), though some outliers are observed. These outliers are primarily due to the model's limitations in accurately capturing cloud dynamics under varying weather conditions, which affect the forecasted UVI values. The right panel of Figure 1 illustrates the frequency distribution of the forecast bias in UVI units, calculated as the difference between forecasted and measured UVI. While there is a concentration of data near zero bias, the distribution is skewed slightly towards positive values, indicating a tendency for UVI overestimation from the model. This is reflected in a positive mean bias error (MBE) of 0.14 (or 4.87%). The Root Mean Square Error (RMSE) for this period is 0.67 (22.77%), reflecting a moderate level of forecast uncertainty. Nevertheless, approximately 80% of the forecast-measurement differences fall within 0.5 UVI units (±20%) range (see Table 1), indicating an overall good performance of the UVI forecasting system. The majority of UVI differences are between ±1 unit as can be seen in Table 1.

Table 1. Distribution of Percentage and Actual Differences Between Forecasted and Measured UVI Values for All Sky Conditions

Relative Differences interval (%)	Relative frequency of occurrence (%)	Absolute Differences interval	Relative frequency of occurrence (%)
±5	38.77	±0.25	67.94
±10	64.37	±0.5	81.16
±20	79.82	±1	92.43

3.2 UVI Clear-sky conditions

Under clear-sky conditions, the accuracy of CERYFOS forecasts improves significantly, as demonstrated in Figure 2, which compares the forecasted and measured UVI for these conditions, showing a strong correlation between predictions and ground-truth data, with minimal deviation. The histogram in Figure 2 (right panel) shows the frequency distribution of forecast-measurement differences under clear-sky conditions, revealing a narrower distribution compared to all-sky conditions. This reduced variability indicates improved precision in UVI forecasts for clear skies. However, the skewness towards positive values is more pronounced, with a MBE of 0.17 (or 4.89%), suggesting a consistent overestimation of forecasted UVI values. The RMSE for this subset is lower, at 0.36 (10.28%), with nearly all differences (~96%) falling within the ±20% range (Table 2). Nevertheless, the 97% of UVI differences are between ±1 UVI units as can be seen in Table 2. Factors contributing to this model overestimation are further examined in Section 3.3.

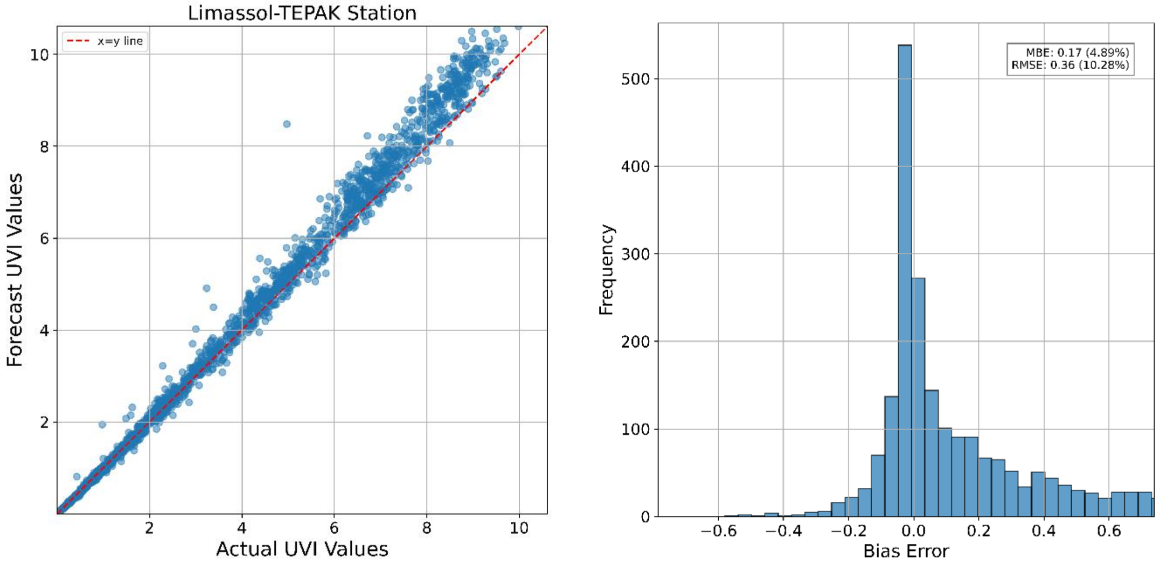

Figure 2. Comparison between forecasted and measured UV Index (UVI): (Left panel) Scatter plot of forecasted versus measured UVI values, and (Right panel) frequency distribution of the Bias Error (forecasted - measured) for the period of December 2023 to September 2024, for clear sky conditions.

Table 2. Distribution of Percentage and Actual Differences Between Forecasted and Measured UVI Values for Clear Sky Conditions

Relative Differences interval (%)	Relative frequency of occurrence (%)	Absolute Differences interval	Relative frequency of occurrence (%)
±5	48.20	±0.25	71.80
±10	80.13	±0.5	85.25
±20	95.73	±1	97.03

3.3 Performance Assessment of Key Influencing Factors

To further explore the factors affecting UVI forecast accuracy, we analysed the relationship between UVI discrepancies and key parameters such as aerosol optical depth (AOD) and ozone variability. The forecasted AOD values were obtained from the Copernicus Atmosphere Monitoring Service (CAMS) and compared with ground-based measurements from the Aerosol Robotic Network (AERONET), both at a wavelength of 550 nm. Forecasted ozone data was retrieved from the Tropospheric Emission Monitoring Internet Service (TEMIS) and compared with actual ozone measurements sourced from the Ozone Monitoring Instrument (OMI) overpass data. Figure 3 illustrates the relationship between the percentage error in the forecasted UV Index (UVI) and the differences between the CAMS forecasted aerosol optical depth (AOD) and

AERONET measurements at 550 nm. The scatterplot is enhanced with a density-based color scale, where red regions indicate areas of higher data point concentration, and blue regions represent sparsely populated areas. The negative slope of the Theil-Sen [16] regression line, with a value of -52.86% per AOD unit, indicates a clear negative correlation between the difference in AOD and the percentage difference in UVI. This implies that when CAMS underestimates AOD, the CERYFOS UVI forecast overestimates the real UVI. Notably, most data points cluster in the negative AOD difference range, signifying that CAMS frequently predicts lower AOD values compared to AERONET measurements. Consequently, this leads to higher UVI predictions, consistent with findings discussed in Sections 3.1 and 3.2. The majority of AOD differences fall within -0.1 units, which, based on the regression slope, corresponds to an average UVI error of approximately -5%. This aligns well with the percentage errors reported in Tables 1 and 2. Figure 4 explores the dependency of UVI forecast error on ozone deviations, with a similar density-based visualization. The Theil-Sen regression line slope of -0.15% per Dobson Unit (DU) suggests a modest negative correlation between the ozone difference and the UVI error. Underestimations in model-predicted ozone generally correspond to overestimations in UVI, and the relationship holds across the observed range of ozone deviations. The data also show that forecasted ozone values are typically higher than the observed measurements, with most differences ranging between -5 and +20 DU. Both figures demonstrate that the accuracy of UVI forecasts is significantly affected by variations in aerosol and ozone levels. Larger discrepancies in AOD or ozone predictions lead to greater errors in UVI forecasts, underscoring the importance of accurate aerosol and ozone modelling for reliable UVI predictions.

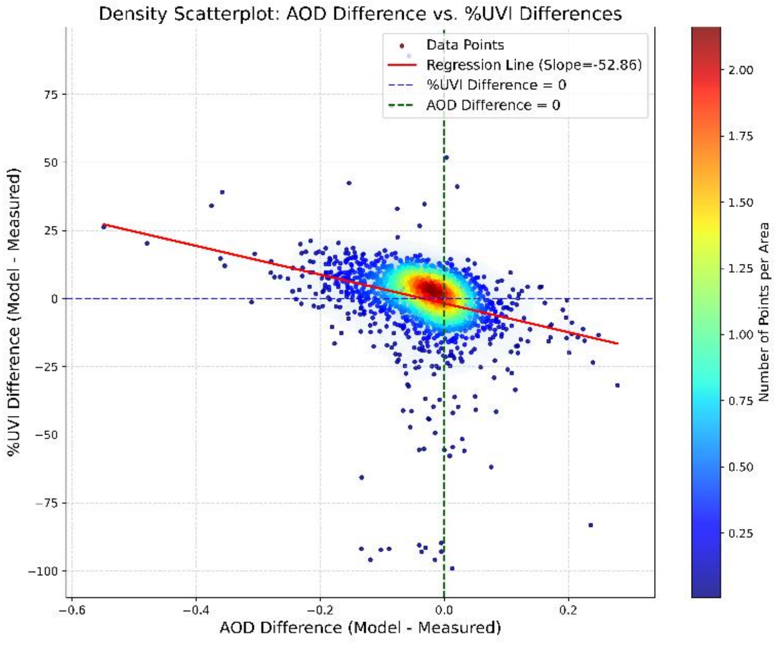

Figure 3. Density Scatterplot: AOD Difference vs. %UVI Differences.

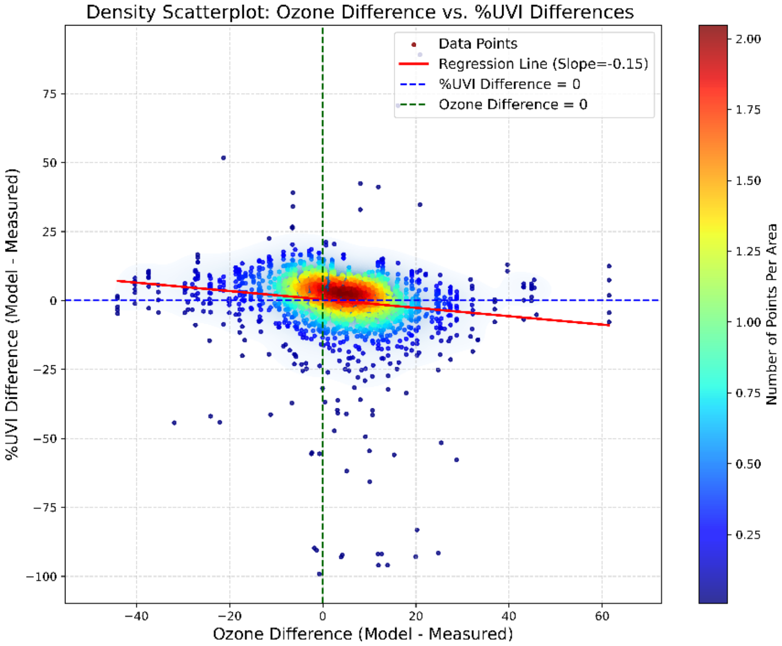

Figure 4. Density Scatterplot: Ozone Difference vs. %UVI Differences.

3.4 Comparative Analysis of UVI Forecast Accuracy with Actinometer and Bentham Spectrophotometer Measurements

Figure 5 depicts the diurnal cycle of forecasted UVI values from the CERYFOS model under all-sky conditions (blue line) for August 28, 2024, along with UVI measurements obtained from two ground-based instruments: a Kipp & Zonen SUV-E radiometer (orange line) and a double monochromator Bentham DMc150 spectrophotometer (green dots). The SUV-E actinometer data provides ground-based UVI measurements, which serve as a direct reference for assessing ultraviolet radiation at the Earth's surface, aiding in real-time validation of the forecasting model's performance. The Bentham spectrophotometer data (green dots), with its high spectral resolution, provides a more precise reference for evaluating the spectral accuracy and radiative transfer reliability of both SUVE measurements and UV forecasts.

Notably, SUV-E measurements show a strong alignment with the Bentham spectrophotometer values, indicating the reliable performance of the SUV-E instrument. Some minor discrepancies (max: 0.5 UVI units difference) arise due to the assumption that ozone levels remain constant throughout the day in the spectral mismatch correction process, as well as the model's omission of aerosol effects. As highlighted in the *2.3* section, both instruments adhere to strict calibration protocols and traceability standards, ensuring that measurement uncertainties remain minimal. For this specific day, forecasted UVI values exhibit an underestimation compared to both SUVE and Bentham measurements. At around 10:00 UTC, coinciding with local solar noon at the Limassol station, the percentage difference between the model and measured UVI is -4.99%, corresponding to an overestimation of the forecasted AOD of 14.67% (0.022 AOD difference) and an overestimation in the forecasted ozone of 6.41% (18.94 DU). This combined influence—a substantial overestimation in AOD and a smaller overestimation in ozone — collectively contributed to the model's underestimation of UVI by -4.99%. This example highlights the importance of accurately predicting both aerosol and ozone concentrations in UVI forecasting models, as significant deviations in either AOD or ozone can considerably affect UVI forecast accuracy.

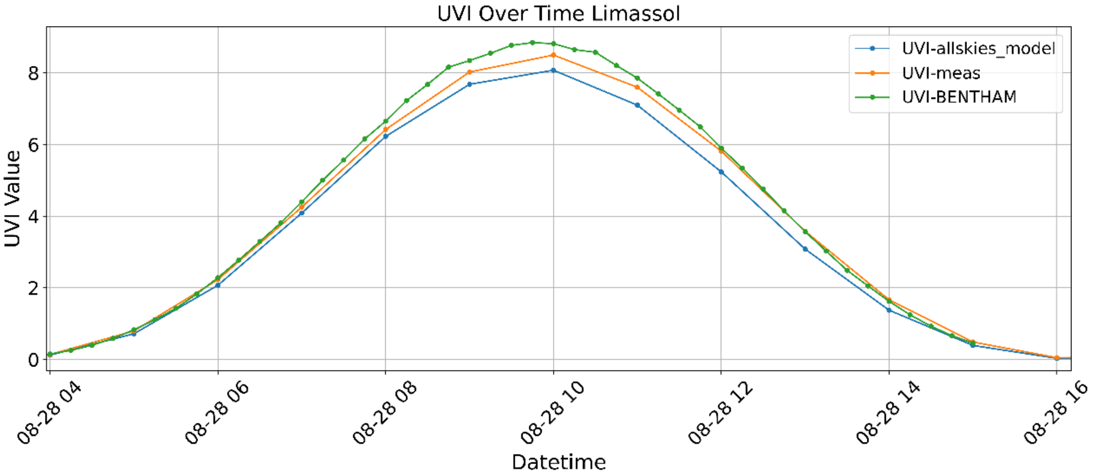

Figure 5. Daily cycle of UV-Index as depicted from different sources (e.g. SUVE actinometer (orange line and dot), Bentham (green line) and modelled (blue all sky conditions).

4. Conclusions

This study presents a preliminary evaluation of the Cyprus Erythemal Irradiance Forecasting System (CERYFOS), designed to provide hourly UV Index (UVI) forecasts across Cyprus. The evaluation covered a nine-month period, from December 2023 to September 2024, and included a detailed comparison between forecasted UVI values and ground-based measurements from a network of Kipp & Zonen SUV-E actinometers and a high-precision Bentham DMc150 double monochromator spectrophotometer.

The results indicate that the CERYFOS model performs well under clear-sky conditions, with a RMSE of 0.36 and a bias of 0.17 UVI units, respectively. However, a consistent overestimation of forecasted values is observed. This overestimation is primarily attributed to the use of aerosol properties, such as AOD and SSA at 550 nm, in the radiative transfer (RT) calculations, as these values tend to be lower than those at relevant UV wavelengths. A future update of the system will address this by incorporating AOD and SSA at 340 nm to enhance accuracy in UV forecasting.

Under all-sky conditions, model performance decreases, with an RMSE of 0.67 UVI units. This increased error highlights the challenges of accurately predicting cloud impacts, which can significantly affect UVI prediction accuracy. Additionally, the study examined the influence of key atmospheric factors, including AOD and ozone column variability, on forecast accuracy. The analysis revealed that forecast discrepancies tend to increase with higher AOD values and significant ozone deviations, underscoring the need for more precise input parameters and improved atmospheric representation.

The comparative analysis between modelled and measured UVI values demonstrates a strong overall correlation, particularly under clear-sky conditions, affirming the robustness of the

CERYFOS model. However, the identified limitations suggest that future enhancements should focus on improving cloud prediction capabilities, integrating localized atmospheric data, and refining aerosol characterization to reduce prediction errors under variable sky conditions.

Author contributions

Conceptualization: GC, KF and SK; ground-based data analysis: GC, KF, IF, AN and SK; Satellite data analysis: KP, and IF; data provision and curation: KF, DHand SK; model parameterization: KP, and SK; model simulations: GC and KF; resources: GC, IF, KF, KP and AN; first draft writing: GC, KF and IF; visualization: GC and KF; writing, review, and editing: all authors, funding acquisition, D.H. All authors gave final approval for publication.

Acknowledgements

The authors acknowledge the EXCELSIOR: ERATOSTHENES: Excellence Research Centre for Earth Surveillance and Space-Based Monitoring of the Environment H2020 Widespread Teaming project (www.excelsior2020.eu, accessed on 13 March 2023). The EXCELSIOR project has received funding from the European Union's Horizon 2020 Research and Innovation Programme under Grant Agreement No 857510, from the Government of the Republic of Cyprus through the Directorate General for the European Programmes, Coordination and Development and the Cyprus University of Technology.

References

[1] World Health Organization (WHO). Radiation: The ultraviolet (UV) index Retrieved April 10, 2023, from: https://www.who.int/uv/faq/ radiation-the-ultraviolet (uv)-index.htm
[2] Neale, R.E., Lucas, R.M., Byrne, S.N. et al. The effects of exposure to solar radiation on human health. Photochem Photobiol Sci 22, 1011–1047 (2023). https://doi.org/10.1007/s43630-023-00375-8
[3] Dolin PJ. Ultraviolet radiation and cataract: a review of the epidemiological evidence. Br J Ophthalmol. 1994 Jun;78(6):478-82. doi: 10.1136/bjo.78.6.478. PMID: 8060933; PMCID: PMC504827.
[4] Bernard, J.J., Gallo, R.L. & Krutmann, J. Photoimmunology: how ultraviolet radiation affects the immune system. Nat Rev Immunol 19, 688–701 (2019). https://doi.org/10.1038/s41577-019-0185-9
[5] Schmalwieser, A. W., Gröbner, J., Blumthaler, M., Klotz, B., De Backer, H., Bolsée, D., ... & O'Hagan, J. UV Index monitoring in Europe. *Photochemical & Photobiological Sciences*, *16*(9), 1349-1370. (2017)
[6] Kyprianou, D., Charalambidou, I., Famojuro, O., Wang, H., Su, D., & Farazi, P. A.. Knowledge and attitudes of cypriots on melanoma prevention: is there a public health concern?. *BMC public health*, (2022)*22*(1), 53.
[7] Emde, C., Buras-Schnell, R., Kylling, A., Mayer, B., Gasteiger, J., Hamann, U., Kylling, J., Richter, B., Pause, C., Dowling, T., and Bugliaro, L.: The libRadtran software package for radiative transfer calculations (version 2.0.1), Geosci. Model Dev., 9, 1647–1672, https://doi.org/10.5194/gmd-9-1647-2016, 2016.
[8] Mayer, B. and Kylling, A.: Technical note: The libRadtran software package for radiative transfer calculations - description and examples of use, Atmos. Chem. Phys., 5, 1855–1877, https://doi.org/10.5194/acp-5-1855-2005, 2005.
[9] Peuch, V., and Coauthors, 2022: The Copernicus Atmosphere Monitoring Service: From Research to Operations. Bull. Amer. Meteor. Soc., 103, E2650–E2668, https://doi.org/10.1175/BAMS-D-21-0314.1.
[10] Rémy, S., Kipling, Z., Huijnen, V., Flemming, J., Nabat, P., Michou, M., Ades, M., Engelen, R., and Peuch, V.-H.: Description and evaluation of the tropospheric aerosol scheme in the Integrated Forecasting System (IFS-AER, cycle 47R1) of ECMWF, Geosci. Model Dev., 15, 4881–4910, https://doi.org/10.5194/gmd-15-4881-2022, 2022.
[11] Eskes, H. J., Van Velthoven, P. F. J., Valks, P. J. M., and Kelder, H. M.: Assimilation of GOME total-ozone satellite observations in a three-dimensional tracer-transport model, Q. J. R. Meteorol. Soc., 129, 1663–1681, https://doi.org/10.1256/qj.02.14, 2003.
[12] Charalampous, G., Fragkos, K., Karpasitis, A., Fountoulakis, I., Nisantzi, A., Papachristopoulou, K., Hadjimitsis, D., & Kazadzis, S. Cyprus Erythemal Radiation Forecasting System (CERYFOS). In IGARSS 2024-2024 IEEE International Geoscience and Remote Sensing Symposium (pp. 3668-3672). IEEE, 2024. 10.1109/IGARSS53475.2024.10642077
[13] Fragkos, K., Nisantzi, A., Fountoulakis, I., Michaelides, S., Charalampous, G., Papachristopoulou, K., Kontoes, C., Hadjimitsis, D., & Kazadzis, S. Introducing the Solar Radiation and Energy Laboratory of the Eratosthenes' Centre of Excellence: Overview of activities. Environmental Sciences Proceedings. 2023;26(1):45. https://doi.org/10.3390/environsciproc2023026045

[14] Webb, A., J. Gröbner, and M. Blumthaler. A Practical Guide to Operating Broadband Instruments Measuring Erythemally Weighted Irradiance, Office for Official Publications of the European Communities, 2006, 21 pp., ISBN 92-898-0032-1
[15] Fountoulakis, I., Diémoz, H., Siani, A. M., Hülsen, G., and Gröbner, J.: Monitoring of solar spectral ultraviolet irradiance in Aosta, Italy, Earth Syst. Sci. Data, 12, 2787–2810, https://doi.org/10.5194/essd-12-2787-2020, 2020.
[16] Theil, H. A rank-invariant method of linear and polynomial regression analysis, I. Proc. Kon. Ned. Akad. v. Wetensch.A53, 386-392. (1950).